Strong nuclear couplings as a source of Coulomb rainbow suppression

N. Keeley,[1,*] N. Alamanos,[2] K. W. Kemper,[3] and K. Rusek[4,1]

[1]*Department of Nuclear Reactions, The Andrzej Sołtan Institute for Nuclear Studies, ul. Hoża 69, PL-00-681 Warsaw, Poland*

[2]*CEA Saclay DSM/IRFU/DIR, F-91 191 Gif-sur-Yvette Cedex, France*

[3]*Department of Physics, Florida State University, Tallahassee, Florida 32306, USA*

[4]*Heavy Ion Laboratory, University of Warsaw, ul. Pasteura 5A, PL-02-093 Warsaw, Poland*

(Received 9 July 2010; published 16 September 2010)

A recent measurement of the ^{11}Be + ^{64}Zn quasielastic scattering angular distribution exhibits a non-Fresnel-type pattern, in contrast to ^{6}He + ^{64}Zn elastic scattering but similar to that for the elastic scattering of ^{6}He from heavy targets. We show by means of continuum discretized coupled-channels (CDCC) calculations that this unusual behavior of ^{11}Be is caused by the much greater importance of nuclear coupling to the continuum in ^{11}Be compared to ^{6}He, where Coulomb dipole coupling is mainly responsible for the non-Fresnel-like shape, when present. We also show that the dynamic polarization potentials derived from the CDCC calculations seem to follow a universal form as a function of radius.

DOI: 10.1103/PhysRevC.82.034606 PACS number(s): 25.60.Bx, 25.60.Je, 24.10.Eq, 25.70.Bc

I. INTRODUCTION

Elastic scattering of heavy ions from heavy targets at incident energies around the Coulomb barrier was shown in early measurements to have a characteristic shape that is remarkably independent of the internal structure of both the projectile and the target (see Ref. [1] for a convenient collection of such measurements). The angular distribution of the differential elastic scattering cross section follows the Rutherford formula out to some angle where one observes a pattern of Coulomb-nuclear interference giving rise to a peak above the Rutherford value, followed by a rapid falloff in cross section as the scattering angle increases. By analogy with the scattering of light, this characteristic shape is often referred to as Fresnel scattering, and the Coulomb-nuclear interference peak as the Coulomb "rainbow." High-precision measurements were required to observe slight differences between isotopes, such as that between ^{6}Li and ^{7}Li + ^{208}Pb elastic scattering [2]. The observation of an anomalously large interaction cross section for ^{11}Li [3] led to the concept of "halo" nuclei, and it was widely speculated that elastic scattering of this nucleus and other possible halo nuclei such as ^{6}He might show anomalous scattering patterns because of the neutron "tail" in their matter distributions. At roughly the same time, polarized Li elastic scattering results demonstrated the importance of virtual coupling to excited states of these weakly bound nuclei [4–6].

With the advent of intense beams of ^{6}He it became possible to obtain high-quality elastic scattering angular distributions for the ^{6}He + ^{197}Au and ^{208}Pb systems that showed highly irregular scattering patterns compared to those of "normal" heavy ions [7–10]. The Coulomb rainbow was completely washed out and the derived optical model parameters were quite different from those found for ^{6}Li scattering. This difference in scattering patterns was shown through continuum discretized coupled-channels (CDCC) calculations to arise from strong virtual E1 Coulomb excitation of the ^{6}He continuum occurring owing to the low binding energy of this nucleus [7]. A subsequent measurement of the elastic scattering of ^{6}He from ^{64}Zn [11] found "normal" angular distributions, demonstrating the need for the large Coulomb field of a target such as ^{208}Pb to generate the strong continuum excitation that produces the anomalous scattering pattern (see also the discussion in Ref. [12]).

A recent article by Di Pietro *et al.* [13] presents angular distributions for the elastic scattering of ^{9}Be, ^{10}Be, and ^{11}Be from a ^{64}Zn target at a center-of-mass energy $E_{\mathrm{c.m.}} \approx 24.5$ MeV. Unlike the ^{9}Be and ^{10}Be + ^{64}Zn angular distributions, which both exhibit the characteristic Fresnel shape with its rainbow peak, the ^{11}Be data show a complete absence of this effect. On the contrary, the ^{11}Be + ^{64}Zn angular distribution drops significantly below the Rutherford value in the angular region where the rainbow peak would be expected in a fashion qualitatively similar to that for ^{6}He elastic scattering from heavy targets. Similar data have been reported for the ^{11}Be + ^{120}Sn system at an incident energy of 32 MeV [14], although over a limited angular range owing to difficulties in separating ^{10}Be fragments from scattered ^{11}Be ions.

In light of the ^{6}He + ^{64}Zn results [11], the strong continuum coupling that must be occurring in the ^{11}Be + ^{64}Zn elastic scattering seems to contradict the earlier conclusions concerning the crucial role of strong Coulomb excitation in effacing the usual Fresnel pattern of the near-barrier angular distribution. This result would then seem to arise from *nuclear* coupling to the continuum, which was found to be relatively weak in the case of ^{6}He. The specific properties of ^{11}Be that could be responsible for this change in form of the elastic scattering are excitation of the low-lying (0.32-MeV) bound first excited state of ^{11}Be, breakup of ^{11}Be via the $^{11}\mathrm{Be} \rightarrow {}^{10}\mathrm{Be} + n$ process and transfer reactions, specifically the ^{64}Zn(^{11}Be,^{10}Be)^{65}Zn stripping process, which should be favored by the long "tail" of the valence neutron wave function (see, e.g., the calculations in Ref. [15]).

We investigate these questions by means of CDCC calculations employing a $^{10}\mathrm{Be} + n$ cluster model of ^{11}Be. The

*keeley@fuw.edu.pl

trivially equivalent local potentials (TELPs) [16] derived from these calculations are compared to help establish the relative importance of Coulomb and nuclear couplings. We also investigate the effect of coupling to the ^{64}Zn(^{11}Be,^{10}Be)^{65}Zn single-neutron stripping reaction to test whether it has a significant influence on the elastic scattering in the region of the Coulomb rainbow.

II. ELASTIC VERSUS QUASIELASTIC SCATTERING

Before describing the calculations we present a brief excursus on the nature of the data of Di Pietro *et al.* [13]. Because the peak caused by excitation of the 0.32-MeV $1/2^-$ first excited state of ^{11}Be could not be resolved, the ^{11}Be data are actually for quasielastic scattering, as clearly stated by Di Pietro *et al.* Nevertheless, they present the results of a Coulomb excitation calculation showing that the inelastic scattering cross section is negligible compared to the elastic scattering, so the data may be regarded as pure elastic for most purposes. This may at first sight seem somewhat surprising, given the large $B(E1)$ for excitation of this state—the largest known for excitation of a bound state. However, both the relatively high incident energy compared to the nominal Coulomb barrier and the low target atomic number combine to reduce the importance of Coulomb excitation. Additionally, although the inelastic scattering cross section is itself large, it is small when compared angle by angle with the elastic scattering, as is clearly shown in Fig. 1 of Di Pietro *et al.* [13].

The fact that the data are quasielastic rather than pure elastic does have one important consequence, though. It enables us to *a priori* rule out any significant contribution to the anomalous scattering shape from excitation of the 0.32-MeV $1/2^-$ state in ^{11}Be. As illustrated in Ref. [17] for quasielastic scattering of ^{4}He from ^{238}U, even when strong coupling to low-lying excited states does give rise to a marked deviation from the expected Fresnel pattern and its associated Coulomb rainbow for pure elastic scattering, the "adding-back" of the inelastic scattering cross sections to give quasielastic scattering results in a standard Fresnel-type angular distribution. Thus, even if coupling to this state were strong enough to produce such an effect—and the calculation of Di Pietro *et al.* [13] shows that it is not—it would not be apparent in the quasielastic scattering data.

III. THE CALCULATIONS

A ^{10}Be $+ n$ cluster model of ^{11}Be was employed, similar to that in Refs. [18] and [19]. We neglected excitation of the ^{10}Be core and assumed a pure ^{10}Be$(0^+) + n$ cluster structure. While inclusion of excited states of the core, in particular the 3.37-MeV 2^+ state, is important from a nuclear structure point of view, a comparison of standard CDCC calculations with those using the more sophisticated XCDCC formalism, which takes core excitation into account [20], suggests that the simpler model is adequate for our purposes.

The neutron was bound to the ^{10}Be core with a Gaussian potential, defined as

$$V(r) = -V_0 \ \exp[-(r/a)^2]. \quad (1)$$

The width parameter a was fixed by requiring the model to reproduce the measured $B(E1; 1/2^+ \rightarrow 1/2^-)$ value of $0.115\ e^2\ \mathrm{fm}^2$ [21]. The depth of the potential well was adjusted to give the correct binding energy in the case of the bound 0.0-MeV $1/2^+$ and 0.32-MeV $1/2^-$ states and a resonance at the correct energy above the ^{10}Be $+ n$ threshold for the 1.78-MeV $5/2^+$ resonance. In addition to these states, couplings to the $L = 0$, 1, 2, and 3 nonresonant continuum were also included with all allowed couplings, including continuum-continuum and reorientation couplings, up to multipolarity $\lambda = 3$. The nonresonant continuum was divided into bins of constant width in momentum space of $\Delta k = 0.2$ fm^{-1} up to a maximum value $k_{\mathrm{max}} = 0.6$ fm^{-1}. This scheme was suitably modified in the presence of the $5/2^+$ $L = 2$ resonance, modeled as a bin of width $\Delta E = 0.2$ MeV, to avoid double counting. The ^{10}Be $+$ ^{64}Zn and n $+$ ^{64}Zn optical potentials required as input for the cluster-folding procedure used to calculate the ^{11}Be $+$ ^{64}Zn diagonal and transition potentials were taken from Di Pietro *et al.* [13] and Koning and Delaroche [22], respectively. Partial waves up to $\ell = 400\hbar$ were included in the calculations and the numerical integrations were carried out to a radius of 120 fm with a step size of 0.07 fm. All calculations were performed with the code FRESCO [23].

For the calculation that added the ^{64}Zn(^{11}Be,^{10}Be)^{65}Zn single-neutron stripping reaction, we included transitions to the 0.0-MeV 0^+ and 3.37-MeV 2^+ states of ^{10}Be and the states in ^{65}Zn listed in Table I of Ref. [24]. Spectroscopic amplitudes for the ^{10}Be/^{11}Be overlaps were taken from Ref. [25], while those for ^{64}Zn/^{65}Zn were taken from Ref. [26]. Coupling between the 0^+ and the 2^+ states of ^{10}Be was included in the exit partition, and the $B(E2)$ and δ_2 values, defining the Coulomb and nuclear coupling strengths, respectively, were taken from Refs. [27] and [28]. The exit partition ^{10}Be $+$ ^{64}Zn optical potential was taken from Ref. [13], although because of the inclusion of the ^{10}Be $0^+ \rightarrow 2^+$ coupling, the real and imaginary well depths were altered to recover the fit to the corresponding elastic scattering data, resulting in values of $V = 145.2$ MeV and $W = 30.8$ MeV.

IV. RESULTS

In Fig. 1 we compare the results of calculations including coupling to the ^{11}Be $1/2^-$ first excited state only (2 channels), couplings to the full ^{10}Be $+ n$ continuum model space (24 channels), and the full breakup coupling scheme plus coupling to the ^{64}Zn(^{11}Be,^{10}Be)^{65}Zn single-neutron stripping reaction with the quasielastic scattering data of Di Pietro *et al.* [13]. Note that the cross section scale is linear rather than the usual logarithmic, to emphasize the region where the Coulomb rainbow would normally occur. The curves denote the calculated quasielastic scattering angular distributions, obtained from the sum of the elastic and inelastic scattering cross sections. The overall description of the data by the full CDCC calculation is reasonable, the agreement up to an angle of $\theta_{\mathrm{c.m.}} \approx 45^\circ$ being excellent, with the calculation overpredicting the data at larger angles. Addition of the single-neutron stripping coupling slightly improves the agreement at angles around $\theta_{\mathrm{c.m.}} \approx 35^\circ$ but increases the cross section for $\theta_{\mathrm{c.m.}} > 50^\circ$, leading to a somewhat worse description

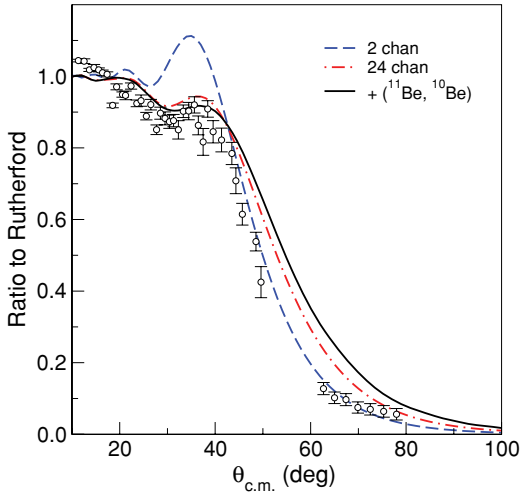

FIG. 1. (Color online) Quasielastic scattering angular distributions for a calculation including coupling to the 0.32-MeV $1/2^-$ state of ^{11}Be only (dashed curve), the full CDCC calculation (dot-dashed curve), and a calculation including the full breakup model space plus the ^{64}Zn(^{11}Be,^{10}Be)^{65}Zn single-neutron stripping (solid curve). Data of Di Pietro *et al.* [13] are denoted by the circles. Note the linear cross-section scale.

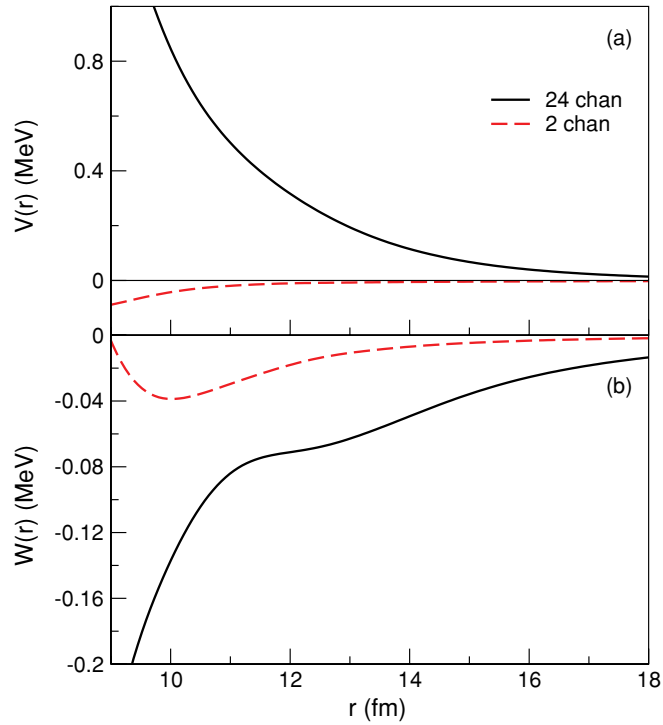

FIG. 2. (Color online) Real (a) and imaginary (b) parts of the TELP DPPs for the 2-channel (dashed curves) and full CDCC (solid curves) calculations from $r = 9$ to $r = 18$ fm.

of the data for these angles. This result may seem rather surprising, as it might reasonably be expected that adding extra reaction channels would lead to increased absorption and hence a reduction in the elastic scattering cross section. However, the backward angle increase in the elastic scattering cross section is a common feature of transfer couplings in this incident energy regime—somewhat above the barrier—as shown by the calculations presented in Ref. [15], for example. The overprediction for $\theta_{\text{c.m.}} > 45^\circ$ may reflect the limitations of neglecting core excitation in our cluster-folding model of ^{11}Be. However, it is clear from the level of agreement obtained—without parameter adjustment—that the simplified model contains the essential physics of the problem and is therefore adequate for our purposes.

It is possible to obtain good agreement with the data over the whole angular region by adjusting the parameters of the ^{10}Be and $n + {}^{64}$Zn potentials used as input to the ^{11}Be cluster-folding potentials. However, as we are concerned here with effects in the region of Coulomb-nuclear interference, we have not done so, as the results of the full calculation plotted in Fig. 1 already provide an excellent description of this angular range. Consequently, parameter adjustment was not considered necessary in the context of our investigation.

It is immediately apparent from Fig. 1 that, as expected, coupling to the ^{11}Be 0.32-MeV $1/2^-$ state alone does not account for the non-Fresnel-type shape of the quasielastic data: in fact, the two-channel quasielastic angular distribution plotted as the dashed curve in Fig. 1 is graphically indistinguishable from the pure elastic scattering of a no-coupling calculation, in complete agreement with the conclusions of Di Pietro *et al.* [13]. We therefore conclude that the main cause of this phenomenon is coupling to the $^{10}\text{Be} + n$ continuum, with a small—almost-negligible—contribution from single-neutron stripping, the main effect of which is to increase the backward angle cross section, in agreement with the calculations for the $^{11}\text{Be} + {}^{208}$Pb system presented in Ref. [15]. Thus far we appear to have a situation similar to ^{6}He elastic scattering from heavy targets.

In Fig. 2 we compare the TELP dynamic polarization potentials (DPPs) for the two-channel and full CDCC calculations in the surface region. The first thing to note is that coupling to the ^{11}Be 0.32-MeV $1/2^-$ state alone provides an almost-negligible contribution to the DPP. The second thing to note is that the DPP is qualitatively similar to that for $^6\text{He} + {}^{208}$Pb (see, e.g., Ref. [29]) in that it is absorptive and repulsive in the surface (the strong absorption radius for the $^{11}\text{Be} + {}^{64}$Zn system at $E_{\text{c.m.}} \approx 24.5$ MeV is about 9.4 fm, defined according to the quarter point recipe) with the absorption continuing out to very large radii. This appears to be more or less universal behavior, see Ref. [17], even down to the shape of the DPPs as a function of radius. However, unlike the $^6\text{He} + {}^{208}$Pb case or the systems examined in Ref. [17], the real part of the DPP only exhibits an extremely weak (about 0.002-MeV) attractive tail at much larger radii, $r > 21$ fm (see also Fig. 4).

The negligible effect of coupling to the ^{11}Be 0.32-MeV $1/2^-$ state belies the large cross section, 240 mb in the full CDCC calculation compared to a total reaction cross section of 2383 mb. It is something of a paradox that coupling to a channel that provides 10% of the total reaction cross section does not produce at least a significant absorptive contribution to the imaginary part of the DPP. A similar case is the $^8\text{B} \rightarrow {}^7\text{Be} + p$ breakup [30,31], underlining the fact that the magnitude of the cross section is not a reliable guide in assessing the importance of coupling to a particular channel or group of channels.

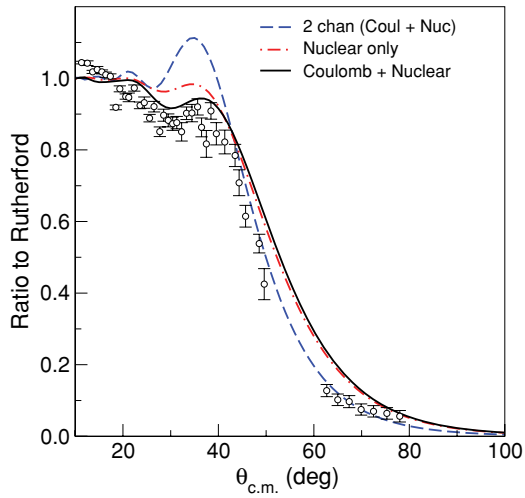

FIG. 3. (Color online) Full model space CDCC calculations with both Coulomb and nuclear couplings, as in Fig. 1 (solid curve), and with nuclear couplings only, but including the diagonal Coulomb potentials (dot-dashed curve). The two-channel quasielastic scattering angular distribution is also included for reference (dashed curve). Note the linear cross-section scale.

Having established that the large coupling effect is almost exclusively caused by breakup, in Fig. 3 we show the effect of switching off the Coulomb excitation on the calculated quasielastic scattering: in the calculation labeled "nuclear only" only the diagonal Coulomb potentials in each channel are retained.

Figure 3 clearly shows that it is the *nuclear* coupling that is mainly responsible for the large coupling effects seen in the measured angular distribution, *including the suppression of the Coulomb rainbow peak,* although the addition of the Coulomb coupling does make a significant contribution in the angular range $25^\circ \leqslant \theta_{\mathrm{c.m.}} \leqslant 40^\circ$. This is in contrast to the situation for the ^{6}He + ^{209}Bi system, where it was found that Coulomb coupling dominates completely over nuclear coupling in suppressing the Coulomb rainbow (see, e.g., Ref. [32]). Note that the conclusions in Ref. [33] for the ^{6}He + ^{197}Au and ^{208}Pb systems as to the importance of nuclear breakup coupling do not contradict Ref. [32], as they refer to the effect of coupling in general—at backward angles the nuclear couplings are most important, as indeed they are for the ^{11}Be + ^{64}Zn data under discussion here. What we wish to emphasize is that for ^{6}He scattered by heavy targets, the Coulomb breakup couplings are vital to the suppression of the Coulomb rainbow—it does not occur when they are switched off—whereas for ^{11}Be they are not, the nuclear breakup couplings alone being sufficient to produce the bulk of this effect.

In Fig. 4 we show the DPPs for full (nuclear plus Coulomb coupling), nuclear-coupling-only, and Coulomb-coupling-only calculations at large radii. Note that the Coulomb-only calculations are pure Coulomb, with no nuclear potentials at all, either diagonal or coupling. At smaller radii the DPP owing to Coulomb coupling alone is negligible compared to that caused by the full calculation or the nuclear-coupling-only calculation. However, as Fig. 4 shows, the Coulomb coupling is responsible for the weak attractive tail for $r > 22$ fm and

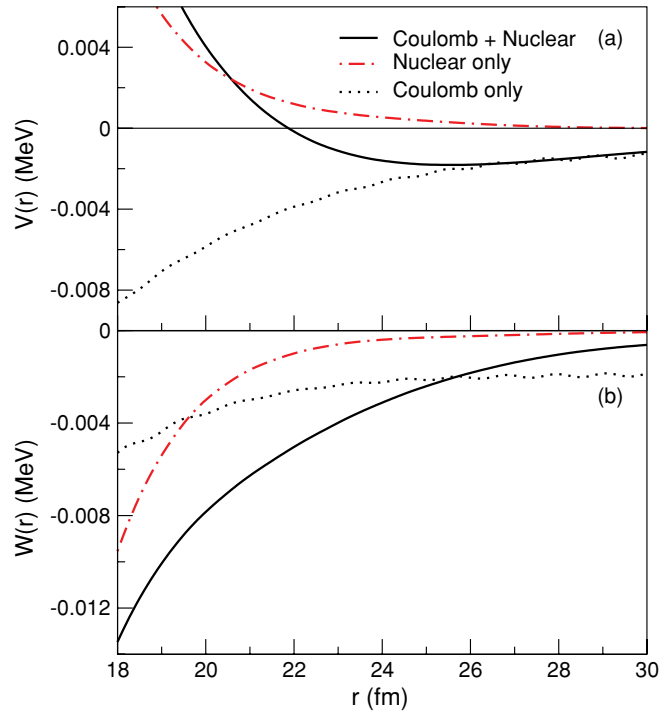

FIG. 4. (Color online) Real (a) and imaginary (b) parts of the TELP DPPs for the calculations of nuclear + Coulomb coupling (solid curves), nuclear coupling only (dot-dashed curves), and Coulomb coupling only (dashed curves) at large radii.

is also the dominant cause of the weak but very long-range absorptive tail for $r > 24$ fm. This is similar to the ^{6}He + ^{208}Pb case, where the long-range attractive and absorptive tail of the DPP is caused by Coulomb dipole excitation [29].

V. CONCLUSIONS

The ^{11}Be + ^{64}Zn quasielastic scattering angular distribution of Di Pietro *et al.* [13] shows the complete lack of a Coulomb rainbow, unlike ^{6}He + ^{64}Zn elastic scattering [11] but similar to that for ^{6}He + ^{197}Au, ^{208}Pb, and ^{209}Bi [7–10]. This suppression of the Coulomb rainbow peak has been found to be characteristic of strong $E1$ Coulomb coupling to the continuum in the case of ^{6}He scattered from heavy targets, a specific manifestation of a more general strong Coulomb coupling effect. However, the relatively light target (for a ^{6}He projectile the Coulomb field of a ^{64}Zn target is manifestly too weak to show the strong Coulomb coupling effect) suggests that possibly strong *nuclear* coupling may be a contributing, if not dominant, factor for ^{11}Be.

Through a series of CDCC calculations we have shown that the most important source of the non-Fresnel-like shape of ^{11}Be + ^{64}Zn quasielastic scattering is indeed nuclear coupling, as it is able to account for the majority of the effect by itself, although Coulomb coupling is still needed to obtain the best description of the data at angles around the Coulomb rainbow peak. Coupling to the ^{64}Zn(^{11}Be, ^{10}Be)^{65}Zn single-neutron stripping was found to have a small effect in the region of the rainbow peak, its main influence being to increase the

backward-angle quasielastic scattering cross section. These conclusions are supported by the TELP DPPs calculated using the wave functions from the CDCC calculations.

However, the incident ^{11}Be energy—$E_{\mathrm{c.m.}} \approx 24.5$ MeV—is relatively high compared to the nominal Coulomb barrier for the ^{11}Be + ^{64}Zn system: 17.96 MeV according to the systematics in Ref. [34]. It is therefore possible that Coulomb coupling effects could become important as the incident energy is reduced toward the Coulomb barrier. We therefore performed two series of CDCC calculations at values of $E_{\mathrm{c.m.}} = 18.77$ and 15.35 MeV (corresponding to laboratory frame energies of 22 and 18 MeV, respectively) to investigate this possibility. These calculations were in all respects identical to those already described for $E_{\mathrm{c.m.}} = 24.5$ MeV, the number of partial waves being reduced to $230\hbar$ and $200\hbar$ at $E_{\mathrm{c.m.}} = 18.77$ and 15.35 MeV, respectively with the matching radii also reduced as appropriate.

The results are presented in Fig. 5. It is apparent from Fig. 5 that while Coulomb breakup coupling does indeed make a more important contribution to producing a non-Fresnel scattering pattern as the incident energy is reduced toward the Coulomb barrier, nuclear coupling retains its importance, still being capable, alone, of completely effacing the Coulomb rainbow at $E_{\mathrm{c.m.}} = 18.77$ MeV. We also note that coupling to the 0.32-MeV $1/2^-$ first excited state also begins to have a noticeable effect on the calculated *elastic* scattering angular distribution as the incident energy is lowered, but as noted, the

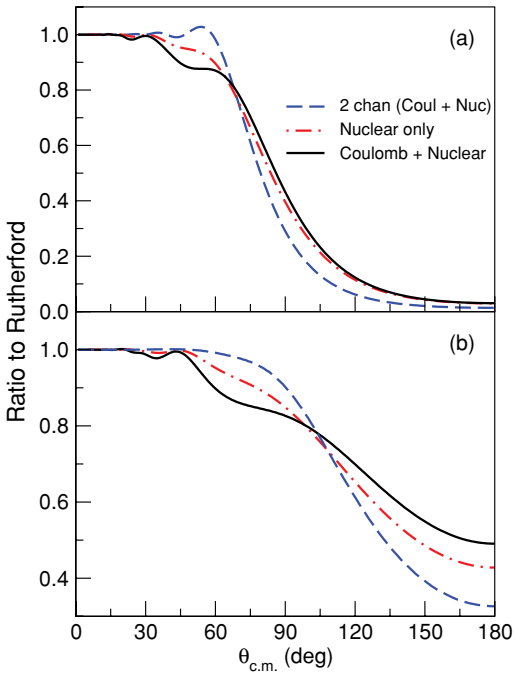

FIG. 5. (Color online) Calculated ^{11}Be + ^{64}Zn quasielastic scattering at (a) $E_{\mathrm{c.m.}} = 18.77$ MeV and (b) $E_{\mathrm{c.m.}} = 15.35$ MeV. Full model space CDCC calculations with both Coulomb and nuclear couplings (solid curve) and with nuclear couplings only, but including the diagonal Coulomb potentials (dot-dashed curve). The two-channel quasielastic scattering angular distribution is also included for reference (dashed curve). Note the linear cross-section scale.

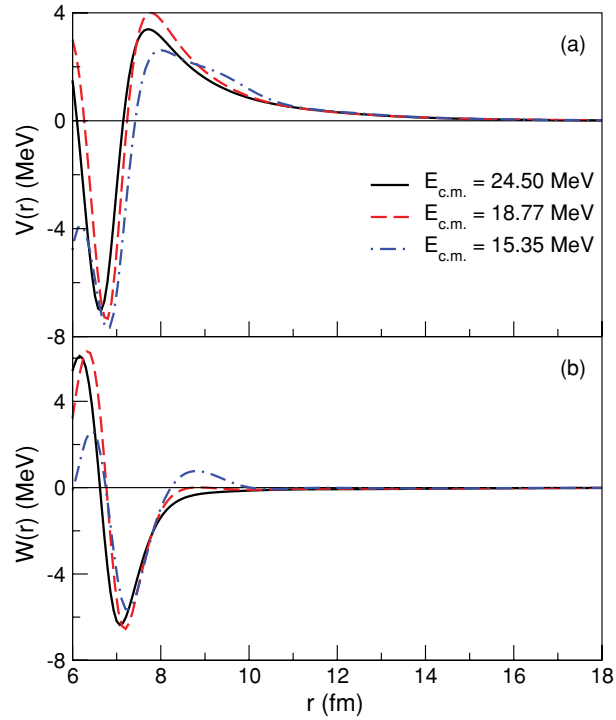

FIG. 6. (Color online) (a) Real and (b) imaginary parts of the TELP DPPs for the full CDCC calculations at $E_{\mathrm{c.m.}} = 24.5$ MeV (solid curves), 18.77 MeV (dashed curves), and 15.35 MeV (dot-dashed curves).

"add-back" effect leads to the two-channel quasielastic scattering angular distributions being virtually indistinguishable from the respective no-coupling elastic scattering.

In Fig. 6 we show the DPPs for the three energies in the nuclear surface region. While there are differences in detail—in particular, the small emissive region around $r \sim 9$ fm at $E_{\mathrm{c.m.}} = 15.35$ MeV—the DPPs at all three energies exhibit the same general form. It should be emphasized that while the DPP can be emissive over small radial ranges—usually owing to the fact that the DPPs we present here are local representations of intrinsically nonlocal objects (see, e.g., Ref. [29])—the total imaginary potential is always absorptive, and unitarity is never violated.

In summary, we conclude that the surprising non-Fresnel-like pattern of ^{11}Be + ^{64}Zn quasielastic scattering is caused by the greater importance of nuclear coupling effects compared to ^{6}He, where such anomalous scattering patterns are only manifest for systems involving heavy targets, owing to the predominance of Coulomb coupling in causing this effect. Although the importance of Coulomb coupling in the ^{11}Be + ^{64}Zn system does increase as the incident energy is reduced toward the Coulomb barrier, nuclear coupling effects remain important, again, in contrast to ^{6}He. The DPP generated by the breakup couplings exhibits the same characteristics as those presented by Rusek [17] for several systems. It therefore seems likely that these characteristics are, in broad outline, truly universal, with the breakdown of the DPP into its component parts, that is, which couplings are the most important contributors, depending on the detailed nuclear

structure of the projectile and/or target nuclei. As beams of more exotic radioactive nuclei with more complex structures (preventing detailed modeling of breakup, for example) are becoming available, it would be useful to attempt to find a simple parametrization of this "generic" DPP form in terms of easily definable nuclear quantities such as $B(E\lambda)$ and breakup threshold. The present work provides a contribution to the systematic study of DPPs from systems that can be realistically modeled that will be needed before such a parametrization can be made.

ACKNOWLEDGMENTS

The authors would like to thank Dr. A. Di Pietro for providing the ^{11}Be + ^{64}Zn data in tabular form. This work was supported by the COPIGAL LEA and by Grant No. N202 033637 from the Ministry of Science and Higher Education of Poland. K.W.K. acknowledges the support of the State of Florida in this work. N.K. would like to thank the Service de Physique Nucléaire of the CEA Centre de Saclay for hospitality during part of the period in which this work was performed.

[1] G. R. Satchler and W. G. Love, Phys. Rep. **55**, 183 (1979).
[2] N. Keeley, S. J. Bennett, N. M. Clarke, B. R. Fulton, G. Tungate, P. V. Drumm, M. A. Nagarajan, and J. S. Lilley, Nucl. Phys. A **571**, 326 (1994).
[3] I. Tanihata, H. Hamagaki, O. Hashimoto, Y. Shida, N. Yoshikawa, K. Sugimoto, O. Yamakawa, T. Kobayashi, and N. Takahashi, Phys. Rev. Lett. **55**, 2676 (1985).
[4] H. Nishioka, R. C. Johnson, J. A. Tostevin, and K. I. Kubo, Phys. Rev. Lett. **48**, 1795 (1982).
[5] H. Nishioka, J. A. Tostevin, and R. C. Johnson, Phys. Lett. B **124**, 17 (1983).
[6] H. Nishioka, J. A. Tostevin, R. C. Johnson, and K.-I. Kubo, Nucl. Phys. A **415**, 230 (1984).
[7] K. Rusek, N. Keeley, K. W. Kemper, and R. Raabe, Phys. Rev. C **67**, 041604 (2003).
[8] O. R. Kakuee *et al.*, Nucl. Phys. A **728**, 339 (2003).
[9] O. R. Kakuee *et al.*, Nucl. Phys. A **765**, 294 (2006).
[10] A. M. Sánchez-Benítez *et al.*, Nucl. Phys. A **803**, 30 (2008).
[11] A. Di Pietro *et al.*, Phys. Rev. C **69**, 044613 (2004).
[12] Y. Kucuk, I. Boztosun, and N. Keeley, Phys. Rev. C **79**, 067601 (2009).
[13] A. Di Pietro *et al.*, Phys. Rev. Lett. **105**, 022701 (2010).
[14] L. Acosta *et al.*, Eur. Phys. J. A **42**, 461 (2009).
[15] N. Keeley, N. Alamanos, K. W. Kemper, and K. Rusek, Prog. Part. Nucl. Phys. **63**, 396 (2009).
[16] I. J. Thompson, M. A. Nagarajan, J. S. Lilley, and M. J. Smithson, Nucl. Phys. A **505**, 84 (1989).
[17] K. Rusek, Eur. Phys. J A **41**, 399 (2009).
[18] K. Hagino, A. Vitturi, C. H. Dasso, and S. M. Lenzi, Phys. Rev. C **61**, 037602 (2000).
[19] A. Diaz-Torres and I. J. Thompson, Phys. Rev. C **65**, 024606 (2002).
[20] N. C. Summers and F. M. Nunes, Phys. Rev. C **76**, 014611 (2007).
[21] D. J. Millener, J. W. Olness, E. K. Warburton, and S. S. Hanna, Phys. Rev. C **28**, 497 (1983).
[22] A. J. Koning and J. P. Delaroche, Nucl. Phys. A **713**, 231 (2003).
[23] I. J. Thompson, Comp. Phys. Rep. **7**, 167 (1988).
[24] N. Keeley and N. Alamanos, Phys. Rev. C **77**, 054602 (2008).
[25] N. Vinh Mau, Nucl. Phys. A **592**, 33 (1995).
[26] E. K. Lin and B. L. Cohen, Phys. Rev. **132**, 2632 (1963).
[27] S. Raman, C. W. Nestor Jr., and P. Tikkanen, At. Data Nucl. Data Tables **78**, 1 (2001).
[28] H. Iwasaki *et al.*, Phys. Lett. B **481**, 7 (2000).
[29] R. S. Mackintosh and N. Keeley, Phys. Rev. C **79**, 014611 (2009).
[30] J. Lubian, T. Correa, E. F. Aguilera, L. F. Canto, A. Gomez-Camacho, E. M. Quiroz, and P. R. S. Gomes, Phys. Rev. C **79**, 064605 (2009).
[31] N. Keeley, R. S. Mackintosh, and C. Beck, Nucl. Phys. A **834**, 792c (2010).
[32] N. Keeley, J. M. Cook, K. W. Kemper, B. T. Roeder, W. D. Weintraub, F. Maréchal, and K. Rusek, Phys. Rev. C **68**, 054601 (2003).
[33] K. Rusek, I. Martel, J. Gómez-Camacho, A. M. Moro, and R. Raabe, Phys. Rev. C **72**, 037603 (2005).
[34] P. E. Hodgson, *Nuclear Heavy Ion Reactions* (Clarendon, Oxford, 1978), p. 2.